Rock physics of hydraulic fractures

Zhishuai Zhang[1], Jing Du[2], and Gary M. Mavko[1]*
[1]Stanford University, [2]Total E&P Research and Technology, LLC

Summary

Both active and passive seismic monitoring of hydraulic stimulation benefit from rock physics knowledge of the seismic signature of hydraulic fractures. The traditional rock physics models for natural fractures may not be a good fit for hydraulic fractures. We started with using Hudson model to investigate how the specific properties of fluid-filled fractures would affect the seismic response of these fractures. Stress effect, scattering effect, squirt flow, and partial saturation were analyzed. Modeling result shows that the creation of fluid-filled fractures will result in changed velocity, anisotropy, and seismic wave attenuation. The rock physics knowledge gained from this study may be used as a starting point to understand field observations as well as to design seismic survey to monitor hydraulic stimulations.

Introduction

The monitoring of hydraulic stimulation is a challenging task. Various seismic data, includes microseismic, time-lapse seismic, seismic imaging, and distributed acoustic sensing (DAS), have been used to achieve this goal (Maxwell, 2014). Tura et al. (2013) have observed the changes in reflection seismic amplitude caused by the creation of fractures or opening of pre-existing fractures associated with injection. Binder et al. (2018) were able to observe delayed P-wave arrivals due to hydraulic stimulation from time-lapse DAS vertical seismic profiling (VSP). Tan et al. (2014) have shown the strong S-wave attenuation due to the stimulated reservoir. Bergery et al. (2015) have proposed a way to infer fluid-filled fractures using both surface and borehole microseismic data. Zhang et al. (2019) have observed increased P-wave attenuation due to hydraulic stimulation. Grechka et al. (2017) and Lin and Zhang (2016) were able to image hydraulic fractures with microseismic data. Riazi and Clarkson (2017) were able to identify hydraulic stimulation induced changes from surface time-lapse seismic survey.

The interpretation of these imaging and characterization results relies on realistic rock physics models. In addition, realistic rock physics model of hydraulic fractures is essential for synthetic earth model building and seismic or microseismic survey design. In most existing works, people use simplified models to explain the field observations and consider only a limited number of factors to explain field observations. Tura et al. (2013) use Kuster and Toksöz (1974a, 1974b)'s model and Cheng (1993)'s model to study the effect of injection induced cracks. Binder et al. (2018) assume that decreased P-wave velocity is mainly the effect of stress change. Riazi and Clarkson (2017) use the Gassmann fluid substitution to model the hydraulic fractures. Though effective to a certain extent, these simplifications need to be further justified by considering various effective of hydraulic fractures comprehensively.

The objective of the work is to gain rock physics knowledge of the seismic response of fluid-filled fractures, which will complement the current seismic technology for hydraulic stimulation monitoring and help to improve the design of this type of seismic surveys.

Theory

We first introduce the Hudson's model and a couple of fluid effects that we studied in this analysis. Though the long wavelength assumption in the effective medium model need to be further validated as shown in the later discussion section, we hope that this treatment will give the first order effect of hydraulic fractures on seismic wave propagation and is a reasonable model to start with. Even most hydraulic fracture planes are perpendicular to the minimum principal stress direction, which makes them to be usually vertical, we treat all the fractures as horizontal planes for simplicity purpose and without loss of generality. The properties of hydraulic fractures along various directions can be achieved by making a rotation to this base model.

Hudson's model

The Hudson's model is based on a scattering formulation analysis of the mean wavefield in an elastic solid with thin, penny-shaped ellipsoidal cracks (Hudson, 1980, 1981). In the Hudson's theory, the second-order interactions between scatters are included but those of the third order are not.

The effective moduli c^{eff} are given as

$$c^{eff} = c^0 + c^1 + c^2, \quad (1)$$

where c^0 is the isotropic background moduli, and c^1 and c^2 are the first- and second-order corrections given by Hudson (1980, 1981). Here, we only use the first order corrections since the second order correction may lead to increasing moduli with crack density beyond the formal limit (Cheng, 1993; Mavko et al., 2009).

Scattering and squirt flow

The high frequency limit of a cracked media saturated with single fluid can be modeled with the Hudson's model with weak inclusions. This assumes the cracks are isolated from each other which makes it lie on the high frequency limit of the squirt effects.

10.1190/segam2019-3216631.1

The low frequency limit can be calculated with two steps. The first step is to compute the dry frame properties with the Hudson's model with weak inclusions. Then, Anisotropic Gassmann fluid substitution can be used to saturate the dry pores with fluid to obtain the low frequency limit of the model.

Partial saturation

For the high frequency effect, the rock properties can be modelled by sequentially using the Hudson's model to calculate the fractured rock saturated with water and gas. This stands for the situation where fluid of various phases is isolated from exchanging under high frequency seismic waves.

The low frequency limit of partial saturation effect can be achieved by the following three steps: First, we can use Reuss average to obtain the properties of water and gas mixture. Then the Hudson's model can be used to calculate the properties of dry cracks. Finally, anisotropic Gassmann fluid substitution can be used to saturate the dry pores with the fluid mixture obtained from the first step.

Characteristic frequencies

Characteristic frequencies of various effects of rocks containing hydraulic fractures and typical reservoir rocks are compared in Figure 1. The effect of hydraulic fractures is to bring the critical frequencies of viscous shear, Biot, and squirt effects to a lower value and bring the patchy saturation to a higher value. All these changes make hydraulic fractures more 'visible' to field seismic survey. Thus, it can be important to consider these effects when building rock physics models for hydraulic fractures.

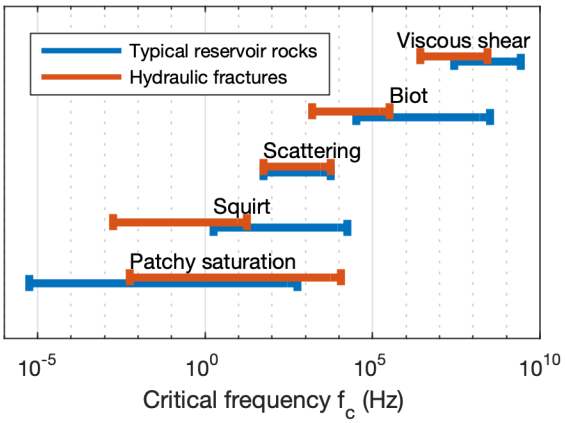

Figure 1: The effect of hydraulic fractures is to bring the critical frequencies of viscous shear, Biot, and squirt effects to a lower value and bring the patchy saturation to a higher value. All of these changes make hydraulic fractures more 'visible' to field seismic survey.

Stress effect

The stress effect on seismic wave propagation can be modeled with stress induced crack density change and aspect ratio change. In this study, we assume the aspect ratio of cracks stays as constant when effective stress changes. The dependence of crack density on effective stress can be expressed with an exponential function $\varepsilon = \frac{N}{V}a^3 = \frac{3\phi}{4\pi\alpha} = C_1 \exp\left[C_2\left(P_{effecitve} - P_0\right)\right]$, where N is the number of ellipsoids with major axis a within the volume V. C_1 and C_2 are respectively a positive and a negative constant, $P_{effecitve}$ is the effective stress and P_0 is a reference stress. An example of this dependency is shown in Figure 2. As the effective stress increases, some cracks tend to close so the crack density decreases. The fracture porosity can be calculated by assuming the aspect ratio stays as a constant as shown by Figure 2.

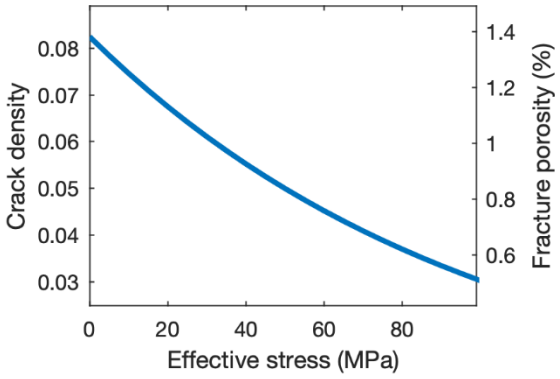

Figure 2: Dependency of crack density and fracture porosity on effective stress. The effect of stress on seismic wave propagation can be modeled with the corresponding crack density change. $C_1 = 0.1$, $C_2 = -10^{-8}\ Pa^{-1}$, $P_0 = 50\ MPa$, $\alpha = 0.02$.

Effects of scattering and squirt flow

The dependence of Thomsen parameters on effective stress in low and high frequency limit is shown on Figure 3. As expected, the vertical propagating P- and S-wave velocities go larger as the effective stress go larger. The P-wave velocity of the dry frame is significantly smaller than the high frequency limit of the saturated media. Saturating the dry frame with fluid brings the velocities to values near the values of high frequency velocities. The Thomsen parameters tend to be smaller as the effective stress increases, which close the cracks. The parameter ε displays significant dispersion while δ and γ do not.

There is no dispersion for S-wave and little dispersion for vertically propagating P-wave. Thus, the attenuation due to squirt effect can be insignificant.

10.1190/segam2019-3216631.1

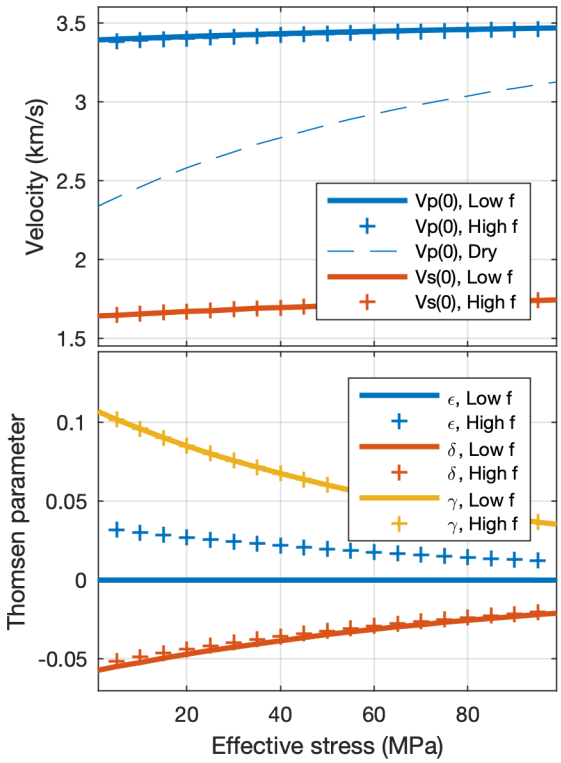

Figure 3: Dependence of Thomsen parameters on effective stress. As the effective stress increase, the velocities of vertical propagating P- and S-waves increase, and the anisotropic parameters decreases. There is no dispersion for S-wave and the dispersion effect of vertically propagating P-wave is insignificant.

Effects of aspect ratio and crack density

Fracture aspect ratio α and crack density ε are the two important parameters to characterize hydraulic fractures. The effects of aspect ratio and crack density on Thomsen parameters are shown on Figure 4. From these maps, we may find that the velocities tend to decrease, and the anisotropic parameters tend to increase with increase in either crack density or aspect ratio. The Thomsen parameters that controls the P-wave propagation (Vertical propagating Vp, ε, and δ) are dependent on both crack density and aspect ratio. However, those controlling S-wave propagation (Vertical propagating Vs and γ) are only sensitive to crack density but are barely affected by aspect ratio.

We may also investigate the dependence of Thomsen parameters on crack density and aspect ratio under the constraint of constant fracture porosity. The fracture porosity induced by a hydraulic stimulation can be expressed by $\phi = \frac{4\pi\alpha\varepsilon}{3}$. The constant porosity contours overlain the Thomsen parameters in Figure 4. Tracing along a constant porosity line, we may find that the effect of cracks on seismic wave propagation goes smaller as the aspect ratio goes larger, that is, the shape of cracks goes more like a sphere.

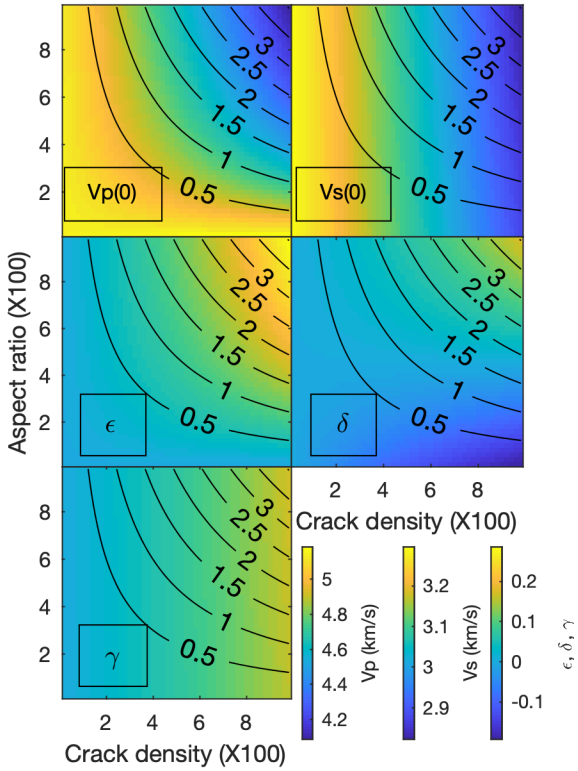

Figure 4: Maps of Thomsen parameters as a function of aspect ratio and crack density. The contour lines are the porosity in percentage.

Effect of partial saturation

The high and low frequency limit of the Thomsen parameters as a function of water saturation are shown by Figure 5. As the water saturation increases, the rock properties change very little in low frequency limit. Under the high-frequency limit, the effect of cracks goes weaker as water saturation increases, which lead to greater dispersion to P-wave.

Attenuation due to partial saturation

The high and low frequency limits of the model can be used for dispersion calculation. Attenuation due to partial saturation can be approximated with a simple standard linear solid model (Mavko et al., 2009) using the dispersion relation predicted previously. The estimated Q values as a function of water saturation for vertically propagating P-wave are shown in Figure 5. The squirt effect and partial saturation won't affect the S-wave attenuation since little dispersion will be predicted for S-wave by the Hudson's

10.1190/segam2019-3216631.1

model. This is consistent with our previous study in the Vaca Muerta formation, where we observed a significant increased P-wave attenuation due to hydraulic stimulation (Zhang et al., 2019). The dispersion estimated Q values explain the change in Qp value due to hydraulic stimulation is larger than the Qs value change.

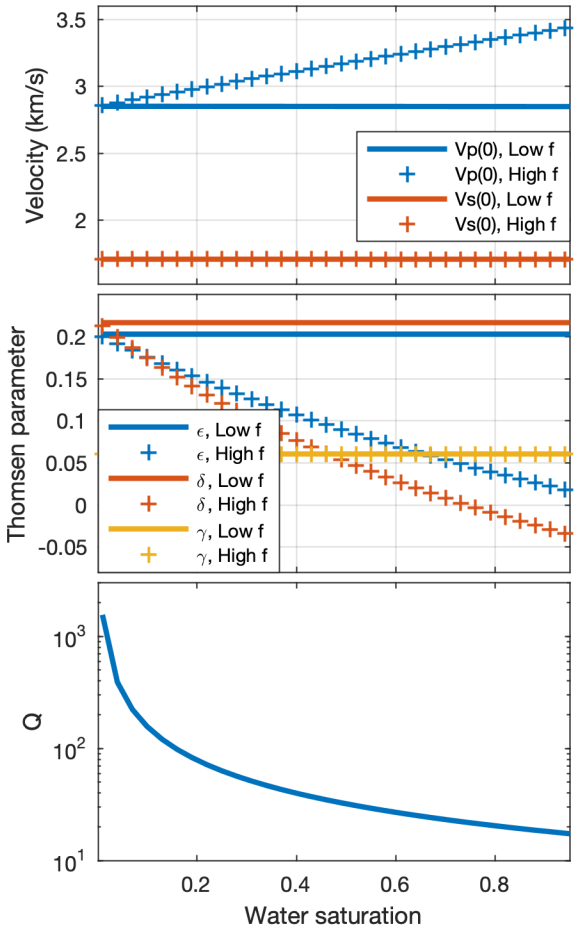

Figure 5: The effect of partial saturation.

Discussion

One of the major limitations of this study may lie in the scale effect. Figure 6 shows the typical geometry size of hydraulic fractures and typical wavelength for various seismic data. According to this comparison, the fracture dimension might be comparable to the seismic wavelength. This makes the underlying long-wavelength assumption of Hudson's model questionable. In this case, other models such as the displacement/velocity discontinuity model (Pyrak-Nolte et al., 1990a, b) may be used to study the hydraulic fracture effect, which will be the next step of this work.

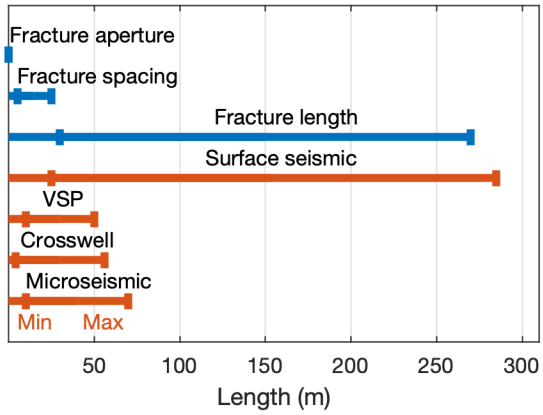

Figure 6: Comparison of the scales of hydraulic fractures and seismic wavelengths.

Conclusions

We studied the effects of stress, scattering, squirt flow, and partial saturation on seismic properties of fluid-filled fractured rocks. The roles of various fracture properties play in seismic wave propagation have been analyzed. We also investigated the seismic properties of fluid-filled fractures in both low- and high-frequency limit. The dispersion under high water saturation condition predicted by this study correspond to significant attenuation of P-waves. Zhang et al. (2019) observed a smaller-than-one Qp/Qs and significant decrease in Qp due hydraulic stimulation in the Vaca Muerta Formation. One possible reason to this phenomenon is due to hydraulic stimulation. The effects discussed in this work provide a possible explanation to this field observation.

Acknowledgments

The authors would like to thank Total for granting permission to publish this paper. This work was done as a post-doc project at Stanford sponsored by Total.

10.1190/segam2019-3216631.1

REFERENCES

Bergery, G., M., Grausem, T., Shuck, and D. E., Diller, 2015, Inferring the presence of fluid-filled fractures using S-wave attenuation on microseismic events: 85th Annual International Meeting, SEG, Expanded Abstracts, 5037–5041, doi: https://doi.org/10.1190/segam2015-5887284.1.

Binder, G., A., Titov, D., Tamayo, J., Simmons, A., Tura, G., Byerley, and D., Monk, 2018, Time delays from stress- induced velocity changes around fractures in a time-lapse DAS VSP: 88th Annual International Meeting, SEG, Expanded Abstracts, 5328–5332, doi: https://doi.org/10.1190/segam2018-2998082.1.

Cheng, C. H., 1993, Crack models for a transversely isotropic medium: Journal of Geophysical Research: Solid Earth, **98**, 675–684, doi: https://doi.org/10.1029/92jb02118.

Grechka, V., Z., Li, B., Howell, H., Garcia, and T., Wooltorton, 2017, High-resolution microseismic imaging: The Leading Edge, **36**, 822–828, doi: https://doi.org/10.1190/tle36100822.1.

Hudson, J., 1980, Overall properties of a cracked solid: Proceedings of Mathematical Proceedings of the Cambridge Philosophical Society.

Hudson, J., 1981, Wave speeds and attenuation of elastic waves in material containing cracks: Geophysical Journal International, **64**, 133–150, doi: https://doi.org/10.1111/j.1365-246X.1981.tb02662.x.

Kuster, G. T., and M. N., Toksöz, 1974a, Velocity and attenuation of seismic waves in two-phase media — Part 1: Theoretical formulations: Geophysics, **39**, 587–606, doi: https://doi.org/10.1190/1.1440450.

Kuster, G. T., and M. N., Toksöz, 1974b, Velocity and attenuation of seismic waves in two-phase media — Part 2: Experimental results: Geophysics, **39**, 607–618, doi: https://doi.org/10.1190/1.1440451.

Lin, Y., and H., Zhang, 2016, Imaging hydraulic fractures by microseismic migration for downhole monitoring system: Physics of the Earth and Planetary Interiors, **261**, 88–97, doi: https://doi.org/10.1016/j.pepi.2016.06.010.

Mavko, G., T., Mukerji, and J., Dvorkin, 2009, The rock physics handbook: Tools for seismic analysis of porous media: Cambridge University Press.

Maxwell, S., 2014, Microseismic imaging of hydraulic fracturing: Improved engineering of unconventional shale reservoirs: SEG.

Pyrak-Nolte, L. J., L. R., Myer, and N. G. W., Cook, 1990a, Anisotropy in seismic velocities and amplitudes from multiple parallel fractures: Journal of Geophysical Research: Solid Earth, **95**, 11345–11358, doi: https://doi.org/10.1029/JB095iB07p11345.

Pyrak-Nolte, L. J., L. R., Myer, and N. G. W., Cook, 1990b, Transmission of seismic waves across single natural fractures: Journal of Geophysical Research: Solid Earth, **95**, 8617–8638, doi: https://doi.org/10.1029/JB095iB06p08617.

Riazi, N., and C. R., Clarkson, 2017, The use of time-lapse seismic attributes for characterizing hydraulic fractures in a tight siltstone reservoir: Presented at the Unconventional Resources Technology Conference, doi: https://doi.org/10.15530/urtec-2017-2670158.

Tan, Y., C., Chai, and T., Engelder, 2014, Use of S-wave attenuation from perforation shots to map the growth of the stimulated reservoir volume in the Marcellus gas shale: The Leading Edge, **33**, 1090–1096, doi: https://doi.org/10.1190/tle33101090.1.

Tura, A., Y., HajNasser, B., Keys, and L., Brown, 2013, Seismic detection of fractures from injection illustrated through a field example: The Leading Edge, **32**, 1446–1454, doi: https://doi.org/10.1190/tle32121446.1.

Zhang, Z., J., Du, and G. M., Mavko, 2019, Reservoir characterization using perforation shots: anisotropy, attenuation and uncertainty analysis: Geophysical Journal International, **216**, 470–485, doi: https://doi.org/10.1093/https://doi.org/gjihttps://doi.org//ggy439.